Versatile biologically inspired electronic neuron

Jacobo D. Sitt* and J. Aliaga†

Departamento de Física, Facultad de Ciencias Exactas y Naturales, Universidad de Buenos Aires, Ciudad Universitaria, Pabellón I, (1428) Buenos Aires, Argentina

(Received 7 July 2006; revised manuscript received 18 September 2007; published 28 November 2007)

We present a biologically inspired electronic neuron based on a conductance model. The channels are constructed using linearly voltage controlled field effect transistors. A two channel and a three channel circuit is developed. The dynamical behavior of this system is studied, showing for the two channel circuit either class-I or class-II excitability and for the three channel circuit bursting and spike frequency adaptation. Voltage-clamp-type measurements, similar to the ones frequently used in neuroscience, are employed in order to determine the conductance characteristics of the electronic channels. We develop an empirical model based on these measurements that reproduces the different dynamical behaviors of the electronic neuron. We found that post-inhibitory rebound is present in the two channel circuit. Reliability and precision of spike timing is induced in the three channel circuit by injecting noise in the control variable of the slow channel that provides a negative feedback. The circuit is appropriate for the design of large scale electronic neural devices that can be used in mixed electronic-biological systems.

DOI: 10.1103/PhysRevE.76.051919 PACS number(s): 87.80.Tq, 87.19.La, 87.80.Xa

I. INTRODUCTION

The modeling of the dynamics of neurons and the possibility of interfacing electronic neurons and living tissues has been a growing field of interest in the physics community [1,2]. Neurons, the building blocks of nervous systems, are the most important biological example of excitability. The simplest excitable models can be classified [following Hodgkin and Huxley (HH)] as class I and II [3]. In class-I systems, the transition from excitability to periodic spiking is mediated by a saddle node homoclinic bifurcation (also known as Andronov bifurcation), while in class-II systems this transition takes place through a (degenerate) Andronov-Hopf bifurcation. The oscillations born in saddle node homoclinic bifurcations are of zero frequency, while the ones being born in Andronov-Hopf bifurcations are characterized by frequencies of finite value. Both class-I and class-II excitable neurons are present in nature. Thus, it is important that the same model can have both behaviors depending on the selection of appropriate parameters.

Another important feature of excitable neurons is bursting. A neuron is bursting when it fires a sequence of spikes followed by a period of nonspiking. Typically, bursting appears due to the interaction of fast currents (responsible for the spiking) and slow currents (responsible for the modulation of that spiking).

A contrast in the reliability and precision of spike timing from in-vivo neurons has been described [4]. The temporal pattern of firing was found to be unreliable when the injected current is constant, but highly reliable when the input is "noisy." Recently, this effect has been studied using a deterministic and stochastic version of the HH-type model [6,7]. While the deterministic model is unable to reproduce qualitatively the reliability and precision of spike timing found in the in-vivo neurons, the stochastic version successfully does it.

The construction of a physical device that analogically integrates the functions of a given neuron according to a specific model has been previously analyzed [1,2]. One of the main advantages of using analog electronic devices is that they can be used in mixed electronic-biological systems. Thus, it is possible to use real time presynaptic and postsynaptic biological responses in order to determine the behavior or the electronic neuron [2].

In this work, we report the construction of an electronic device inspired in the HH phenomenological model [3] of action potentials (AP). Our simplified version has circuits that represent characteristic channels, where these channels represent large populations of real biological channels. We developed a persistent, instantaneously activated, sodium channel (Na^+), a slow persistent potassium channel (K^+) and a much slower persistent potassium channel [$K^+(M)$]. The selection of channels respond to the minimal configuration that enables the circuit to reproduce the mentioned features of the dynamics of neurons [8].

The work is organized as follows. Section II presents the electronic neuron and studies the dynamics of the two channel circuit. In Sec. III we study the dynamics of the three channel circuit. A review of firing properties and channels in biological and electronic neurons is presented in Sec. IV. The induction by noise of reliability and precision of spike timing is included in Sec. V. Finally, in Sec. VI we present the conclusions.

II. EXCITABLE SYSTEM: THE TWO CHANNEL ELECTRONIC NEURON DYNAMICS

A. Circuit

The electronic neuron consists in a simple circuit [Fig. 1(a)] inspired in the HH model. In the two channel circuit version the switch s is opened. V_m and V_i are the membrane

*jaco@df.uba.ar
†jaliaga@df.uba.ar

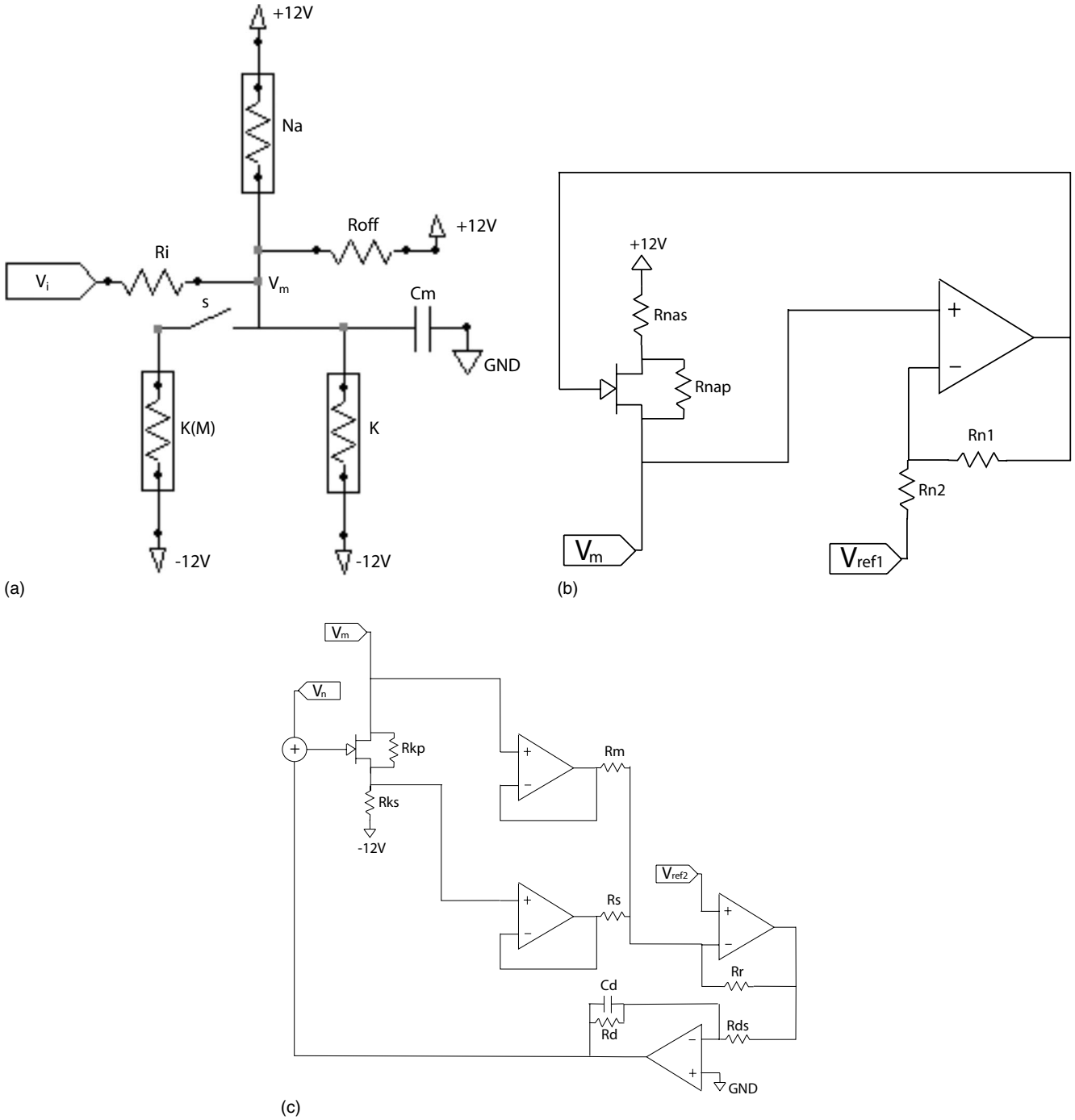

FIG. 1. Electronic neuron: (a) Schematic for the neuron circuit (R_i=39 kΩ, R_{off}=20 kΩ and C_m=47 nF), (b) Na sodium channel (R_{nas}=39 kΩ, R_{nap}=10 kΩ, R_{n1}=100 kΩ, and R_{n2}=50 kΩ), (c) K potassium channel (R_{ks}=20 kΩ, R_{kp}=10 kΩ, R_m=18 kΩ, R_s=39 kΩ, R_r=39 kΩ, R_{ds}=11 kΩ, R_d=11 kΩ, and C_d=100 nF).

and input voltages, respectively, R_i=39 kΩ, R_{off}=20 kΩ, and C_m=47 nF. Sodium (Na^+) and potassium (K^+) channels are constructed using field effect transistors (FETs) acting as voltage controlled resistors (e.g., VCR4N, Vishay siliconix). While the sodium channel is instantaneously activated the potassium channel has relative slower dynamics. The opening delay of this channel is determined by R_d and C_d [schematics for the channels in Figs. 1(b) and 1(c)]. The threshold of the sodium and potassium channels can be modified by changing V_{ref1} and V_{ref2}, respectively. The relationship between these two thresholds determines the type of excitability of the neuron. V_n is the noise input used in Sec. V.

In order to connect the electronic device to biological neurons the voltage scale of both systems must be the same. This can be done by adding an amplifying stage built with operational amplifiers [2].

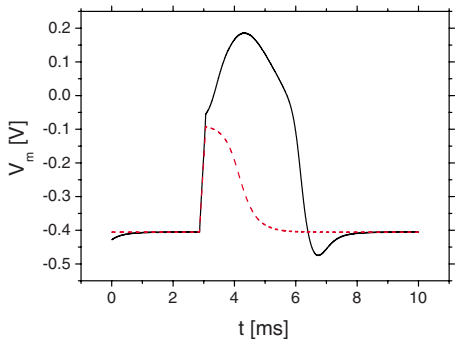

FIG. 2. (Color online) Membrane potential (V_m) for different amplitude square input pulses lasting 200 ms. (Red, dashed line) Subthreshold input amplitude 1000 mV. (Black, solid line) Overthreshold input amplitude 1100 mV.

B. Dynamical tests

In order to evaluate the dynamics of the circuit different tests are performed. To study the excitability square pulses of different amplitudes lasting 200 ms are injected through V_i. Figure 2 shows the response of V_m for subthreshold and over-threshold pulses. We have also injected a sinusoidal forcing signal through V_i and have analyzed the response of V_m as the amplitude and frequency of the injected signal is changed. In Fig. 3 we show the experimental map of the regions in which the different periodical patterns with rotation number $q:p$ (i.e., the time series have q spikes every p periods of the forcing signal) have been observed. The Arnold tongues bend toward higher periods as the forcing amplitude diminishes, as expected for an excitable system.

The different dynamics of both types of classes of excitability can be observed in Fig. 4. We obtained each type of excitability by selecting two different values of V_{ref2}. Figure 4(a) shows the amplitude of the spike for different amplitude square pulses lasting 200 ms injected through V_i. For class-I-type excitability a sharp threshold can be observed while for class II the threshold is, as expected, more smooth. When injecting a constant excitatory input V_i excitability is lost, as previously discussed, and the period of the bearing oscillations classifies the type of excitability. Figure 4(b) shows the period of the oscillations for different dc V_i. For class-I excitability the oscillations are born with an infinite period while for class-II excitability the oscillations are born with finite period, as expected.

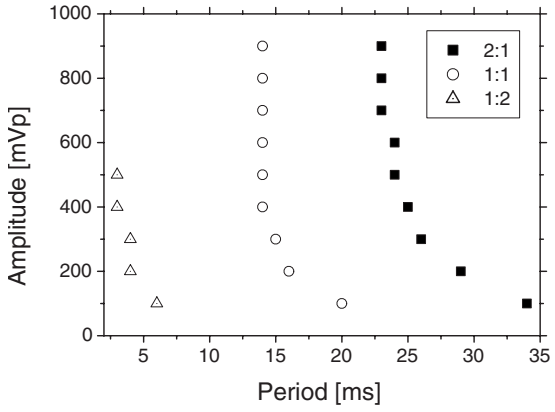

FIG. 3. Rotation numbers $q:p$ (q spikes every p periods of the injected signal) of periodic orbits observed as function of the amplitude and frequency of the external forcing applied.

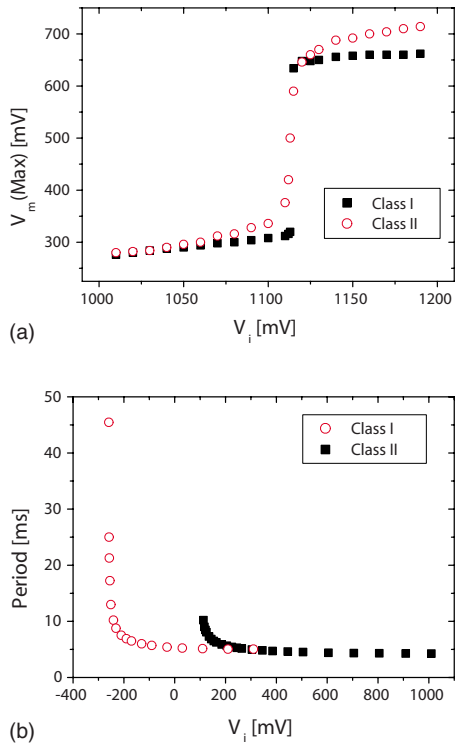

FIG. 4. (Color online) Threshold tests ($V_{\mathrm{ref1}}=2$ V and $V_{\mathrm{ref2}}=1.2$ V in the class-I circuit and $V_{\mathrm{ref1}}=2$ V and $V_{\mathrm{ref2}}=1$ V in the class-II circuit), (a) amplitude of the AP vs amplitude of the input pulse (width 200 ms), (b) period of V_m vs dc V_i input.

C. Post-inhibitory rebound

Post-inhibitory rebound is a nonlinear phenomenon found in a variety of neurons. In this process the excitability of the neuron is enhanced temporarily following a period of hyperpolarization. This phenomenon is present in the electronic neuron (see Figs. 5 and 6). In this process the hyperpolarization pulse inactivates the K^+ current, this inactivation continues briefly after the end of the pulse, due to the time constant of the K^+ channel, enhancing the excitability of the neuron.

D. Model

The dynamics of the electronic neuron can be studied using a conductance-based model built on the measurable variables in our circuit (membrane voltage and currents through the channels).

The dynamics of the membrane potential, V_m, is given by

$$C_m\dot{V}_m = V_i g_i + V^+(g_1 + g_{\mathrm{off}}) - V^- g_2 - V_m(g_{\mathrm{off}} + g_i + g_1 + g_2), \tag{1}$$

where g_i and g_{off} are the inverse of R_i and R_{off}, which biologically represent the input and leak conductance, respec-

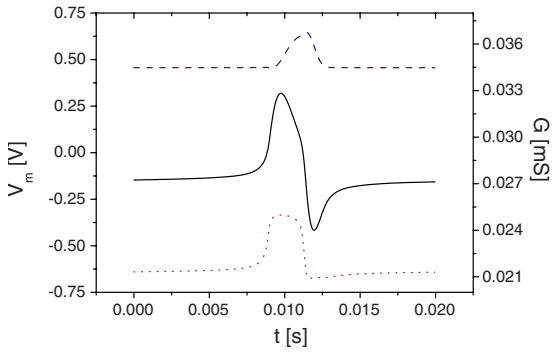

FIG. 5. (Color online) Evolution of the conductance of the sodium (red, dotted line) and potassium channels (blue, dashed line) for a typical spike (black, solid line).

tively, V_i is the input tension, g_1 and g_2 are the conductance of the Na^+ and K^+ channels which are V_m dependent, and V^+ and V^- are the voltages of the dc source (e.g., +12 V and −12 V). Conductance for the channels can be fitted using arbitrary HH-type equations. The conductance of the Na^+ channel reads as

$$g_1 = g_{mi} + m_\infty g_{ma}, \tag{2}$$

where g_{mi} and g_{ma} are constants and the instantaneously activate variable m_∞ is

$$m_\infty(V_m) = \frac{A_m e^{b_m V_m}}{1 + A_m e^{b_m V_m}}, \tag{3}$$

where A_m and b_m are constants. The conductance of the K^+ channel is given by

$$g_2 = g_{ni} + n g_{na}, \tag{4}$$

where g_{ni} and g_{na} are constants and the dynamics of the activating variable n is ruled by

$$\tau(V_m)\dot{n} = -n + n_\infty, \tag{5}$$

where $\tau(V_m)$ is the characteristic time and

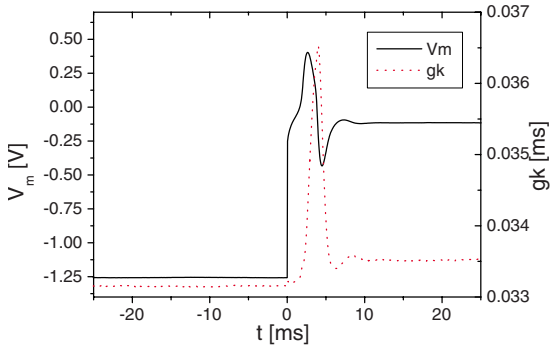

FIG. 6. (Color online) Post-inhibitory rebound. The neuron is hyperpolarized with a pulse of −4 V, 100 ms (end of the pulse t =0 ms). Spike after the pulse (black, solid line). Conductance of the K^+ channel (red, dotted line).

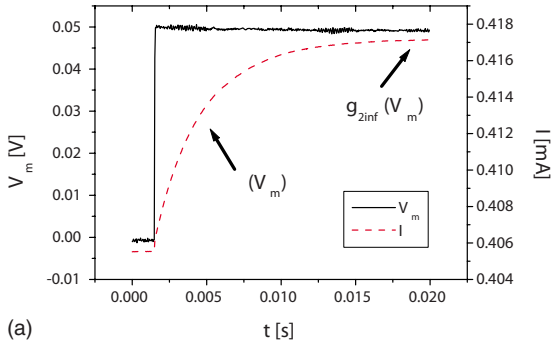

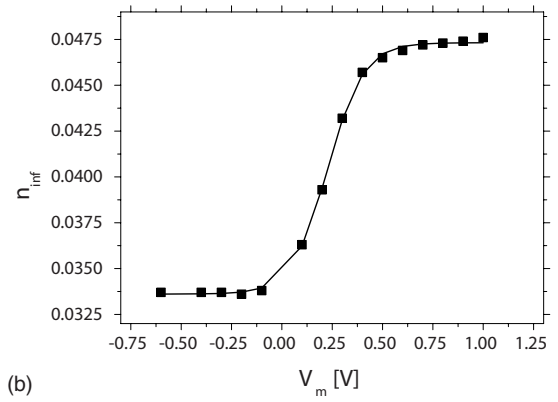

FIG. 7. (Color online) (a) Evolution of the current on the potassium channel (red, dashed line) for a 50 mV step in V_m (black, solid line), (b) activation variable n of the potassium channel vs V_m.

$$n_\infty(V_m) = \frac{A_n e^{b_n V_m}}{1 + A_n e^{b_n V_m}}, \tag{6}$$

where A_n and b_n are constants.

The next section shows how for each type of excitability the dynamics of the channels can be fitted, obtaining different sets of parameters. Using each one of the sets of parameters previously obtained, Eqs. (1)–(5) can be integrated and class-I or class-II excitability is achieved.

E. Voltage-clamp-type measurement

In order to fit our model to the electronic channels dynamical behavior voltage-clamp-type measurements are used. This biological technique is used to study the conductance of a population of membrane channels for different membrane potentials [9]. In this case V_m is clamped using a signal generator and then the conductance of each channel is analyzed. Figure 5 shows the evolution of the conductance of each channel for a typical spike. As the sodium channel is instantaneously activated we fix V_m using a ramp signal and then record the conductance measuring the current through the channel. Because the potassium channel has slower dynamics, a different technique is used to study it. In this case, V_m is fixed using small amplitude steps [see Fig. 7(a)] and for each step the time constant, $\tau(V_m)$, and the steady-state conductance, $g_{2\,\mathrm{inf}}(V_m)$, are determined. With the fitted parameters, the simulation of V_m for an excitatory ramp signal

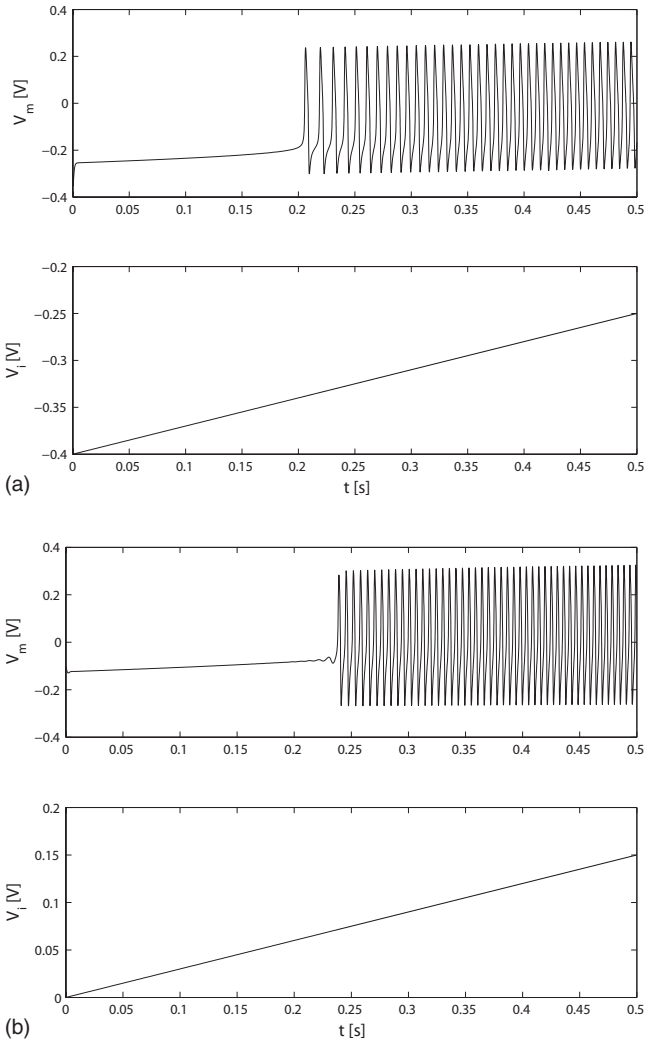

FIG. 8. Simulation of V_m with a excitatory ramp signal: (a) class-I and (b) class-II excitability.

is obtained (see Fig. 8). As expected, the oscillations are born with frequency zero for class I and with frequency of finite value for class II.

III. SPIKE FREQUENCY ADAPTATION AND BURSTING: THE THREE CHANNEL ELECTRONIC NEURON DYNAMICS

Some neurons (i.e., layer 5 pyramidal cells) show a modulation of the instantaneous spiking frequency of a long train of action potentials. This phenomenon is called spike frequency adaptation. Slow currents are responsible for this modulation. Bursting is another typical behavior of neuronal dynamics. Both spike frequency adaptation and bursting phenomena can be modeled by adding a third channel to the model described in the preceding section.

A. Spike frequency adaptation

In order for our circuit to show spike frequency adaptation a very slow K^+ channel $[K(M)]$ must be added to the circuit by closing switch s [see Fig. 1(a)]. The schematic of the $K(M)$ channel is identical to the K^+ used before. The opening delay of this channel is determined by R_d and C_d. This channel will slowly hyperpolarize the neuron thus decreasing the spike rate or even stopping the spiking depending on the amplitude of the input pulse. Figure 9 shows the spike frequency adaptation for a 250 ms input square pulse. The spiking frequency at the beginning and at the end of the pulse depends on the magnitude of the current of $K(M)$ at the closed and open states, respectively.

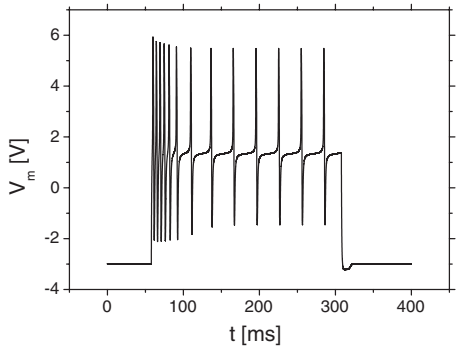

FIG. 9. Spike frequency adaptation. V_m for an input square pulse of 3 V duration 250 ms input square pulse.

A similar modulation phenomena called spike frequency acceleration is present in Cortical fast spiking interneurons. In this case the instantaneous spiking frequency increases for each spike. This can also be obtained in our circuit by adding a slow Na^+ channel (not shown).

B. Bursting

To make the electronic neuron burst the parameters in the two channel circuit must be modified in order for it to present bistability (coexistence of a stable node, representing the resting state, and a limit cycle, representing the spiking state). Figure 10 shows how a short pulse injected in V_i takes the circuit from the stable node to the limit cycle and then a following identical pulse takes it back from the limit cycle to the stable node.

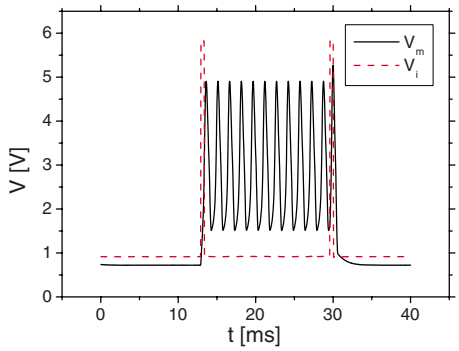

FIG. 10. (Color online) Bistability in the two channel circuit. The circuit presents a stable resting state and a stable spiking state V_m (black, solid line). Alternation between states is produced by injecting a short input pulse (0.6 ms, 5 V) V_i (red, dashed line).

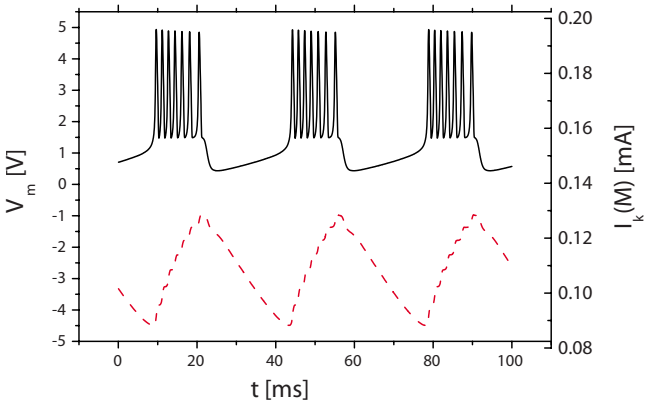

FIG. 11. (Color online) Typical bursting. V_m (black, solid line) and $I_{K(M)}$ current (red, dashed line).

The K(M) current will be responsible to make the circuit oscillate between states. Figure 11 shows a typical bursting activity and the current of the K(M) channel. This channel is inactive during the rest state and slowly activates during the spiking state. As the current through the K(M) channel grows, the circuit becomes less excitable and eventually stops to spike.

IV. FIRING PROPERTIES

The electronic neuron can express the four main firing properties: adaptation, post-inhibitory rebound, oscillations, and delayed excitation [11]. The combination of sodium, potassium, and extra channels are responsible for each one of the properties. The extra channels involved in each firing property for the biological and the electronic neuron are shown in Table I. Post-inhibitory rebound was shown in Sec. II when only the sodium and potassium channel were needed for that property. Adaptation and oscillations were shown in Sec. III when a slow K^+ channel was added. Delayed excitation was not shown but can be obtained by adding a slow Na^+ channel responsible for the delay in crossing the spiking threshold.

V. RELIABILITY AND PRECISION OF SPIKE TIMING INDUCED BY NOISE

Both experimental and theoretical work have shown that, depending on the nature of the input, spike timings in neurons can be precise and reliable [4,5]. One of the key aspects associated with this effect is that in biological neurons ion channels are stochastic devices and the probabilistic gating of these devices adds noise to the membrane voltage in the neuron. Because the number of fluctuating channels is of the order of $\sqrt{N}$ [10], where N is the number of channels, the macroscopic effects of this transitions are more important in the channels with less density population.

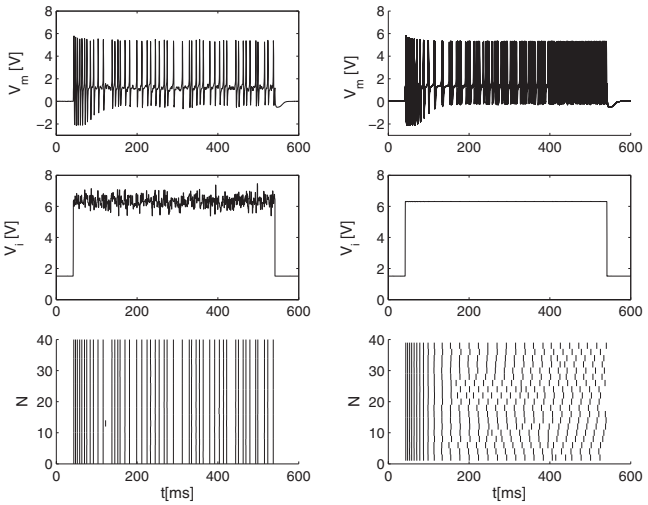

FIG. 12. Comparison of reliability and accuracy with constant (right-hand side) and noisy (left-hand side) input pulses. Top figures are superimposed spikes trains, middle figures are input pulses, and bottom figures are raster plots.

In our model the stochastic effect in the current throughout the channels can be induced by injecting low-pass filtered (τ=1 ms) Gaussian noise in the signal that controls the gating of the FETs in the electronic channels [through V_n in Fig. 1(c)]. In our case, because K(M) is the channel with lower conductance, the stochastic effect is only reproduced in that channel.

Figure 12 shows the different responses to constant and "noisy" (Gaussian σ=120 mV, low pass filtered τ=1 ms) input pulses. As expected, the noisy pulse improves the reliability and accuracy of the spike train.

The peristimulus time histogram (PSTH, not shown) of 19 successive presentations of a particular stimulus was smoothed using an adaptive filter to yield an estimate of the

TABLE I. Firing properties.

Firing property	Biological channels	Electronic channels
Post-inhibitory rebound	H-type current or T-type current [13]	Two channels
Adaptation	Calcium activated potassium channel or muscarinic potassium channels or slow Na^+ deinactivation time constant [12]	Two channels+slow K^+ channel
Oscillations	Calcium current, H current, T current [13]	Two channels+slow K^+ channel
Delayed excitation	A- and D-type potassium current or potassium inward rectifier current [14]	Two channels+slow Na^+ channel

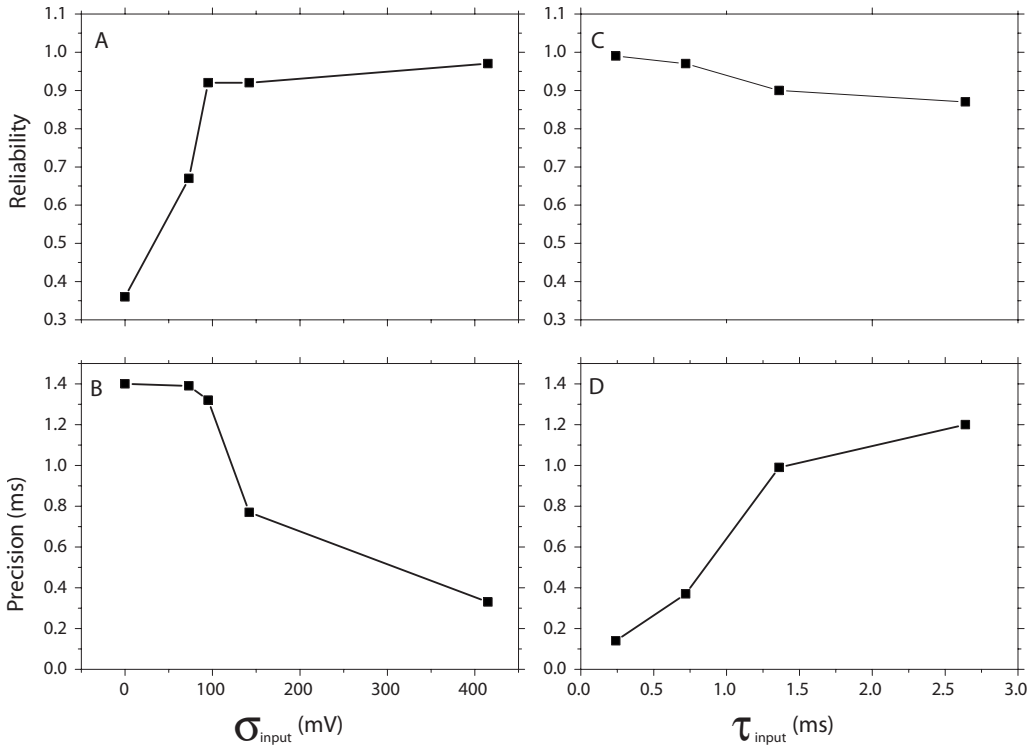

FIG. 13. Dependence of reliability and precision on stimulus parameters. Reliability and precision are calculated using the events of the smoothed PSTH. (a) Reliability of the electronic neuron, for stimulus with fixed time constant and various fluctuation amplitudes ($\tau_{\text{input}}=1$ ms, $\sigma_{\text{input}}=0-400$ mV). (b) Precision of the electronic neuron for the same input as in (a). (c) Reliability of the electronic neuron, for stimulus with fixed fluctuation amplitude and various time constants ($\tau_{\text{input}}=0.2-2.6$ ms, $\sigma_{\text{input}}=120$ mV). (d) Precision of the electronic neuron for the same input as in (c).

instantaneous firing rate. Spikes during the first 300 ms of the stimulus onset, during which most frequency adaptation occurred, were discarded. Significant elevations of the fire rate (events) were selected form the PSTH using a threshold of 3 times the mean firing rate. Reliability is defined as the fraction of total spikes that occur during that event and precision as the standard deviation of spike time within the event.

The correlation of reliability and precision with the amplitude of the fluctuations in the input pulses (σ_{input}) and the time constant of low pass filter were calculated from the PSTH, and are shown in Fig. 13. Consistently with previous results [6] reliability increases with σ and decreases with τ while precision decreases with τ and increases with σ.

VI. CONCLUSIONS

In this work we report the development of an electronic neuron with the capability to express different biological features like class-I and class-II types of excitability, spike frequency adaptation, bursting, and stochastic resonance. Our circuit is a minimal biologically inspired conductance-based model.

The design allows us the study of the dynamics using biological-type techniques, i.e., the measurement of the conductance of the channels in terms of the membrane voltage V_m. This versatile electronic neuron, that is able to reproduce the typical dynamical features of biological neurons, is appropriate for the design of large scale electronic neural circuits.

The use of this electronic neuron and the development of plastic electronic synapses, using voltage controlled resistors, will allow us to generate electronic neural ganglion of nucleus having learning or memory capability. These circuits will be applied in robotics and neural tissue-machine interaction.

ACKNOWLEDGMENTS

This work was partially funded by Fundación Antorchas, UBA, CONICET. One of the authors (J.S.) would like to thank Professor Gabriel Mindlin and Professor R. Pinto for helpful discussions.

[1] R. D. Pinto, P. Varona, A. R. Volkovskii, A. Szücs, H. D. I. Abarbanel, and M. I. Rabinovich, Phys. Rev. E **62**, 2644 (2000); A. Szücs, R. D. Pinto, M. I. Rabinovich, H. D. I. Abarbanel, and A. I. Selverston, J. Neurophysiol. **89**, 1363 (2003); A. Szücs, P. Varona, A. R. Volkovskii, H. D. I. Abarbanel, M. I. Rabinovich, and A. I. Selverston, J. Comput. Neurosci. **2**, 1 (2000); Y. Yarom, Neuroscience **44**, 263 (1991); S. Le Masson, A. Laflaquiere, T. Bal, and G. Le Masson, IEEE Trans. Biomed. Eng. **46**, 638 (1999); M. F. Simoni, G. S. Cymbalyuk, M. Q. Sorensen, R. L. Calabrese, and S. P. DeWeerth, IEEE Trans. Biomed. Eng. **51**, 342 (2004); R. Jung, E. J. Brauer, and J. J. Abbas, IEEE Trans. Neural Syst. Rehabil. Eng. **9**, 319 (2001).

[2] J. Aliaga, N. Busca, V. Minces, G. B. Mindlin, B. Pando, A. Salles, and L. Sczcupak, Phys. Rev. E **67**, 061915 (2003).

[3] A. L. Hodgkin and A. F. Huxley, J. Physiol. **117**, 500 (1952).

[4] Z. F. Mainen and T. Sejnowski, Science **268**, 1503 (1995).

[5] G. A. Cecchi, M. Sigman, J. M. Alonso, L. Martinez, D. R. Chialvo, and M. O. Magnasco, Proc. Natl. Acad. Sci. U.S.A. **97**, 5557 (2000).

[6] E. Schneidman, B. Freedman, and I. Segev, Neural Comput. **10**, 1679 (1998).

[7] P. V. Carelli, M. B. Reyes, J. C. Sartorelli, and R. D. Pinto, J. Neurophysiol. **94**, 1169 (2005).

[8] E. M. Izhikevich, *Dynamical Systems in Neuroscience: The Geometry of Excitability and Bursting* (MIT Press, Massachusetts, 2006).

[9] J. Keener and J. Sneyd, *Mathematical Physiology* (Springer, New York, 1998), Chap. 3.

[10] J. A. White, J. T. Rubinstein, and A. R. Kay, Trends Neurosci. **23**, 131 (2000).

[11] E. R. Kandel, J. H. Schwartz, and T. M. Jessell, *Principles of Neural Science* (McGraw-Hill, New York, 2000).

[12] J. Benda and A. V. M. Herz, Neural Comput. **15**, 2523 (2003).

[13] T. Bal and D. A. McCormick, J. Neurophysiol. **77**, 3145 (1997).

[14] V. Morisset and F. Nagy, Eur. J. Neurosci. **10**, 3642 (1998).